

# Magnetogenesis, spectator fields and CMB signatures

Massimo Giovannini<sup>1</sup>

*Centro “Enrico Fermi”, Compendio del Viminale, Via Panisperna 89/A, 00184 Rome, Italy*

*Department of Physics, Theory Division, CERN, 1211 Geneva 23, Switzerland*

## Abstract

A viable class of magnetogenesis models can be constructed by coupling the kinetic term of the hypercharge to a spectator field whose dynamics does not affect the inflationary evolution. The magnetic power spectrum is explicitly related to the power spectrum of (adiabatic) curvature inhomogeneities when the quasi-de Sitter stage of expansion is driven by a single scalar degree of freedom. Depending upon the value of the slow-roll parameters, the amplitude of smoothed magnetic fields over a (comoving) Mpc scale can be as large as 0.01–0.1 nG at the epoch of the gravitational collapse of the protogalaxy. The contributions of the magnetic fields to the Sachs-Wolfe plateau and to the temperature autocorrelations in the Doppler region compare favourably with the constraints imposed by galactic magnetogenesis. Stimulating lessons are drawn on the interplay between magnetogenesis models and their possible CMB signatures.

---

<sup>1</sup>e-mail address: massimo.giovannini@cern.ch

Since the early fifties large-scale magnetic fields have inspired different areas of investigation both at a theoretical and at a more phenomenological level (see, as an example, Ref. [1] for theoretical and historical accounts of the subject). Both elliptical and spiral galaxies have magnetic fields at the  $\mu$  G level [2]. Abell clusters possess large-scale magnetic fields (not associated with individual galaxies) with typical correlation scale which can be as large as 100 kpc [3]. Superclusters have been also claimed to have magnetic fields [4] at the  $\mu$ G level even if, in this case, crucial ambiguities persist on the way the magnetic field strengths are inferred from the Faraday rotation measurements. The latest analyses of the AUGER experiment demonstrated a correlation between the arrival directions of cosmic rays with energy above  $6 \times 10^{19}$  eV and the positions of active galactic nuclei within 75 Mpc [5]. At smaller energies it has been convincingly demonstrated [6] that overdensities on windows of 5 deg radius (and for energies  $10^{17.9}\text{eV} < E < 10^{18.5}\text{eV}$ ) are compatible with an isotropic distribution. Thus, in the highest energy domain (i.e. energies larger than 60 EeV), cosmic rays are not appreciably deflected: within a cocoon of 70 Mpc the intensity of the (uniform) component of the putative magnetic field should be smaller than the nG. On a theoretical ground, the existence of much larger magnetic fields (i.e.  $\mathcal{O}(\mu\text{G})$ ) cannot be justified already if the correlation scale is of the order of 20 Mpc.

In the late sixties Harrison [7] suggested that cosmology and astrophysics are just two complementary aspects of the origin of large-scale magnetic fields. Heeding observations there is no evidence against the primeval hypothesis even if the primordial origin of large-scale magnetism is not empirically compelling. Compressional amplification (taking place during the gravitational collapse of the protogalaxy) allows to connect the observed magnetic field to a protogalactic field, present prior to gravitational collapse, of typical strength ranging between 0.1 and 0.01 nG. A better understanding of the interplay between dynamo theory and the global conservation laws of magnetized plasmas has been recently achieved also because of the improved comprehension of the solar dynamo action [8]. Within the dynamo hypothesis, the protogalactic field could be even much smaller than the nG and still explain some crucial properties of our magnetized Universe: astrophysical and cosmological mechanisms might really be complementary rather than mutually exclusive [7, 8] (see also [1], second reference).

The only direct way of putting the primordial hypothesis to test is represented by the observations related to the Cosmic Microwave Background <sup>2</sup> (CMB in what follows): the possible existence of a magnetized plasma prior to decoupling is germane to several CMB observables like temperature autocorrelations and cross-correlations (see [9] and references therein). Recently, a semi-analytical technique has been developed to compute more accu-

---

<sup>2</sup>It is not excluded that the study of the morphological features of galactic fields will also give indications, albeit indirect, on the primordial nature of the protogalactic field (see Ref. [2] and discussions therein).

rately than before the magnetized temperature and polarization autocorrelations as well as cross-correlations [10]: the gross logic of the method is to assume a dominant adiabatic mode in the pre-equality initial conditions and to add, consistently, the effects of the magnetic fields in the Einstein-Boltzmann hierarchy and in the initial conditions.

Large-scale magnetic fields produced inside the Hubble radius after inflation will have a correlation scale bounded (from above) by the Hubble radius at the moment when some charge separation is produced (be it, for instance, the electroweak time<sup>3</sup>). Since the Hubble radius, during radiation, evolves much faster than the correlation scale of the produced field, the typical scale over which the magnetic field is coherent today is much shorter than the Mpc, obliterating, in this way, the possibility of successfully reproducing the galactic magnetic field [9]. Conversely, the physical rationale for inflationary magnetogenesis resides on the possibility of achieving large correlation scales: quantum fluctuations of Abelian gauge fields can be amplified in the same way as zero point fluctuations of the geometry are amplified. Unlike the scalar and tensor modes of the geometry, Abelian gauge fields (like the hypercharge) in four space-time dimensions obey Weyl invariant evolution equations [11]. Since the pumping action of the background geometry is not efficient in amplifying the fluctuations of gauge fields, Weyl invariance should be broken for the viability of the whole construction [11]. The amplified gauge fields should be Abelian. The only non-screened vector modes that are present at finite conductivity are the ones associated with the hypercharge field [12]. The non-Abelian fields develop actually a mass and they are screened as the Universe thermalizes. After the electroweak phase transition the photon field remains unscreened with amplitude  $\cos \theta_w \vec{\mathcal{J}}$ . While the coupling of the hypercharge to fermions is chiral, the QED coupling is vector-like. At finite conductivity, however, the descriptions of the two plasmas are similar<sup>4</sup> and can be given in terms of an effective (Ohmic) current which is proportional to the (hyper)electric field. The specific nature of the gauge field is often ignored in the current literature: the main endeavour is to break consistently Weyl invariance (possibly maintaining gauge invariance). The Abelian field arising in this case which should be thought, indeed, as a putative hypercharge field.

In the present paper it will be argued that Weyl invariance can be broken through the coupling of a spectator field to the gauge kinetic term also in the case of conventional inflationary scenarios. A spectator field is defined, in the present context, as a field which does not drive the inflationary evolution but which is, nonetheless, dynamical. It is not excluded, in the present context, that the resulting large-scale magnetic fields are amplified

---

<sup>3</sup>This example holds under the assumption the electroweak phase transition is strongly first order which is, arguably, not the case.

<sup>4</sup>See [12] and the equations of anomalous magnetohydrodynamics, i.e. the generalization of magnetohydrodynamics to the case where anomalous effects are included.

to nG strength and with a nearly scale-invariant spectrum. The field content of the model is apparent from the total action which includes, on top of the gravitational part, the contribution of the inflaton  $\varphi$  and of the spectator field  $\psi$ :

$$S_{\text{tot}} = S_{\text{gravity}} + S_{\varphi} + S_{\psi}. \quad (1)$$

The various components of the total action can be written, in explicit terms, as<sup>5</sup>

$$S_{\text{gravity}} = -\frac{\overline{M}_{\text{P}}^2}{2} \int d^4x \sqrt{-g} R, \quad S_{\varphi} = \int d^4x \sqrt{-g} \left[ \frac{1}{2} g^{\alpha\beta} \partial_{\alpha} \varphi \partial_{\beta} \varphi - V(\varphi) \right], \quad (2)$$

$$S_{\psi} = \int d^4x \sqrt{-g} \left[ \frac{1}{2} g^{\alpha\beta} \partial_{\alpha} \psi \partial_{\beta} \psi - W(\psi) - \frac{\lambda(\psi)}{16\pi} Y_{\alpha\beta} Y^{\alpha\beta} \right], \quad (3)$$

where  $V(\varphi)$  and  $W(\psi)$  are, respectively, the inflaton potential and the potential of the spectator field. The hypercharge field strength  $Y_{\alpha\beta} = \nabla_{[\alpha} Y_{\beta]}$  is defined in terms of the covariant derivative with respect to the four-dimensional metric  $g_{\mu\nu}$ . In Eq. (3),  $\lambda(\psi)$  denotes the coupling of  $\psi$  to the hypercharge field.

In a conformally flat Friedmann-Robertson-Walker metric  $g_{\mu\nu} = a^2(\tau) \eta_{\mu\nu}$  (where  $\eta_{\mu\nu}$  is the four-dimensional Minkowski metric), the Hamiltonian constraint stemming from the equations derived from the total action (1) is given by

$$\overline{M}_{\text{P}}^2 \mathcal{H}^2 = \frac{1}{3} \left[ \frac{\varphi'^2}{2} + V a^2 \right] + \frac{1}{3} \left[ \frac{\psi'^2}{2} + W a^2 \right] + \frac{1}{8\pi} (\vec{\mathcal{B}}^2 + \vec{\mathcal{E}}^2), \quad (4)$$

where the prime denotes the derivation with respect to the conformal time coordinate  $\tau$  and  $\mathcal{H} = a'/a$  is related to the Hubble parameter  $H$  as  $\mathcal{H} = H/a$ . In Eq. (4)  $\vec{\mathcal{E}} = \sqrt{\lambda} \vec{e}$  and  $\vec{\mathcal{B}} = \sqrt{\lambda} \vec{b}$  are, respectively, the hyperelectric and the hypermagnetic fields defined, from the field strength as<sup>6</sup>  $Y_{0i} = a^2 e_i$  and  $Y_{ij} = -a^2 \epsilon_{ijk} b^k$ . The dual field strengths (appearing in the Bianchi identity) are simply  $\tilde{Y}_{ij} = a^2 e^m \epsilon_{mij}$  and  $\tilde{Y}_{0i} = a^2 b_i$ . The field  $\varphi$  is the dominant source of the background geometry while  $\psi$  is a spectator field which is allowed to roll during inflation but which gives a negligible contribution to the background geometry. Denoting by  $\psi_i$  the initial value of  $\psi$  at a curvature scale  $H_i$  this requirement implies that

$$\psi_i^2 < \frac{2}{3} \left( \frac{H_1}{H_i} \right)^2 \overline{M}_{\text{P}}^2 \quad (5)$$

where  $H_1$  is the curvature scale at the end of inflation. When  $\psi$  starts rolling at  $\tau_i$  the hyperelectric and the hypermagnetic fields are just given by their corresponding quantum

---

<sup>5</sup>The conventions on the four-dimensional metric will be mostly minus, i.e.  $(+, -, -, -)$ . Recall also that  $\overline{M}_{\text{P}} = M_{\text{P}}/\sqrt{8\pi}$  with  $M_{\text{P}} = 1.22 \times 10^{19} \text{ GeV}$ .

<sup>6</sup>The rescaling of  $\vec{e}$  and  $\vec{b}$  through  $\sqrt{\lambda}$  arises since the hypercharge energy-momentum tensor contains the coupling to  $\psi$  through  $\lambda$ . These will not be, however, the normal modes of the system as it will be clear in a moment.

fluctuations and are therefore even smaller than the energy density of  $\psi$ . The (homogeneous) evolution equation for  $\psi$  will therefore be given by

$$\psi'' + 2\mathcal{H}\psi' + \frac{\partial W}{\partial \psi}a^2 + \frac{a^2}{8\pi} \frac{\partial \ln \lambda}{\partial \psi}(\vec{\mathcal{B}}^2 + \vec{\mathcal{E}}^2) = 0. \quad (6)$$

The values of the hypermagnetic (and hyperelectric) fields generated from quantum fluctuations will be always smaller than the energy density of  $\psi$ . This implies that the back-reaction terms arising, for instance, in Eqs. (4) and (6) can be safely neglected. It will be assumed that  $W(\psi) = m^2(\psi - \psi_*)/2$  with  $m < H_1$ . Since  $\psi$  is light during inflation, it will also be required that  $\psi_* \ll M_{\text{P}}$ . Deep in the course of the inflationary epoch the evolution equation of  $\psi$  is then

$$\Sigma'' + [\mu^2 - (2 - \epsilon)]a^2 H^2 \Sigma = 0, \quad \Sigma = a\psi, \quad \epsilon = -\frac{\dot{H}}{H^2} = \frac{\overline{M}_{\text{P}}}{2} \left( \frac{V_{,\varphi}}{V} \right)^2 \quad (7)$$

having introduced  $\mu = m/H$  and the first slow-roll parameter  $\epsilon$  which is related to the first derivative of the inflaton potential. In the limit  $\mu \ll 1$  the evolution of  $\psi$  will be simply given by

$$\psi = \psi_{\text{i}} \left( -\frac{\tau}{\tau_{\text{i}}} \right)^\beta + \psi_*, \quad \beta = \frac{3 - 2\epsilon}{1 - \epsilon}. \quad (8)$$

As the field  $\psi$  evolves in time, the hypermagnetic and hyperelectric fields can be parametrically amplified, as it follows from the equations of motion easily obtainable by the appropriate functional variation of the total action (1):

$$\nabla_\mu (\lambda Y^{\mu\nu}) = 4\pi J^\nu, \quad \nabla_\mu (\tilde{Y}^{\mu\nu}) = 0, \quad \lambda(\psi) = \left( \frac{\psi - \psi_*}{\overline{M}_{\text{P}}} \right)^\alpha. \quad (9)$$

where the contribution of the (Ohmic) current  $J^\nu$  has been included for convenience. In Eq. (9) the expression of  $\lambda(\psi)$  contains the parameter  $\alpha$  which will eventually determine the slope of the gauge field spectra and which will be constrained by phenomenological considerations. In the conformally flat metric  $g_{\mu\nu} = a^2(\tau)\eta_{\mu\nu}$ , Eq. (9) can be written, using vector notations, as:

$$\vec{\nabla} \times (a^2 \sqrt{\lambda} \vec{\mathcal{B}}) = \frac{\partial}{\partial \tau} [a^2 \sqrt{\lambda} \vec{\mathcal{E}}] + 4\pi \vec{J}, \quad \vec{\nabla} \cdot \vec{J} = 0, \quad (10)$$

$$\frac{\partial}{\partial \tau} \left[ \frac{a^2 \vec{\mathcal{B}}}{\sqrt{\lambda}} \right] + \vec{\nabla} \times \left[ \frac{a^2 \vec{\mathcal{E}}}{\sqrt{\lambda}} \right] = 0. \quad (11)$$

where  $\vec{J} = a^3 \sigma_c = \sigma a^2 \vec{e} = \sigma a^2 \vec{\mathcal{E}}/\sqrt{\lambda}$ ;  $\sigma(\tau) = \sigma_c a(\tau)$  denotes the rescaled value of the conductivity and it appears because of the choice of the conformal time coordinate as a pivot variable of the system. Since  $\lambda$  depends only upon  $\tau$  the Ohmic current is always divergence-less as it should be by definition. Combining Eqs. (10) and (11) in the absence

of conductivity (i.e. during inflation) the hypermagnetic and hyperelectric fields obey the following pair of (decoupled) equations:

$$\vec{B}'' - \nabla^2 \vec{B} - \frac{(\sqrt{\lambda})''}{\sqrt{\lambda}} \vec{B} = 0, \quad \vec{E}'' - \nabla^2 \vec{E} - \sqrt{\lambda} \left( \frac{1}{\sqrt{\lambda}} \right)'' \vec{E} = 0, \quad (12)$$

where  $\vec{E} = a^2 \vec{\mathcal{E}}$  and  $\vec{B} = a^2 \vec{\mathcal{B}}$  are the normal modes of the system. The dual nature of the pump fields for  $\vec{E}$  and  $\vec{B}$  in Eq. (12) is a reflection of the strong-weak coupling duality of the Abelian theory in the absence of sources (see, for instance, [13]). During inflation the gauge field fluctuations can then be quantized in the Coulomb gauge (which is the appropriate one for treating gauge fields in time-dependent background geometries [14]) and the vector potential can be expanded in terms of the appropriate mode functions  $f_k(\tau)$

$$\hat{\mathcal{Y}}_i(\vec{x}, \tau) = \frac{1}{(2\pi)^{3/2}} \sum_{\gamma} e_i^{(\gamma)} \int d^3k [\hat{a}_{\vec{k}, \gamma} f_k(\tau) e^{-i\vec{k} \cdot \vec{x}} + \hat{a}_{\vec{k}, \gamma}^\dagger f_k^*(\tau) e^{i\vec{k} \cdot \vec{x}}], \quad (13)$$

where  $e_i^{(\gamma)}$  is the polarization unit vector;  $\hat{a}_{k, \gamma}$  and  $\hat{a}_{\vec{p}, \gamma}^\dagger$  obey  $[\hat{a}_{k, \gamma}, \hat{a}_{\vec{p}, \gamma}^\dagger] = \delta_{\gamma\gamma'} \delta^{(3)}(\vec{k} - \vec{p})$ . Since  $\vec{B} = \vec{\nabla} \times \vec{\mathcal{Y}}$ , the mode function  $f_k(\tau)$  (and its complex conjugate) will satisfy the same equation obeyed by  $\vec{B}$  (see Eq. (12)).

At end of inflation the Universe reheats. Thanks to the decay of the inflaton and of the spectator field the quasi-de Sitter background becomes effectively dominated by a fluid of ultra-relativistic particles with radiative equation of state. Overall the plasma is globally neutral but the conductivity becomes large since charged species are copiously produced. Lorentz invariance is then broken and hyperelectric fields are strongly suppressed while the hypermagnetic fields survive. A preferred physical frame naturally emerges, i.e. the so-called plasma frame where the conductivity is finite and the hyperelectric fields are dissipated. Since  $\psi$  decays,  $\lambda$  will freeze and the system of Eqs. (10) and (11) can be written as

$$\frac{\partial \vec{E}_a}{\partial \tau} + 4\pi\sigma \vec{E}_a = \vec{\nabla} \times \vec{B}_a, \quad \frac{\partial \vec{B}_a}{\partial \tau} = -\vec{\nabla} \times \vec{E}_a, \quad (14)$$

where the subscript “a” signifies that the hyperelectric and hypermagnetic fields are computed after the transition to radiation. Denoting with the subscript “b” the field variables after the rise of the conductivity the appropriate continuity conditions for the magnetic and the electric fields are:

$$\vec{B}_a = \vec{B}_b, \quad \vec{E}_a = \frac{\vec{\nabla} \times \vec{B}_a}{4\pi\sigma} = \frac{\vec{\nabla} \times \vec{B}_b}{4\pi\sigma}. \quad (15)$$

Equation (15) stipulates that, after the transition, the electric fields are suppressed by the conductivity as soon as radiation dominates. Solving Eq. (12) during inflation and Eq. (14) during radiation the boundary conditions (15) permit the estimate of the two point

function of the hypermagnetic field operators for a generic time  $\tau > \tau_1$  where  $\tau_1$  denotes the epoch of the sudden rise in the conductivity:

$$\langle 0 | \hat{B}_i(\vec{x}, \tau) \hat{B}_j(\vec{y}, \tau) | 0 \rangle = \int d \ln k P_B(k) P_{ij}(k) \frac{\sin kr}{kr}, \quad r = |\vec{x} - \vec{y}|, \quad (16)$$

where  $P_B(k)$  and  $P_{ij}(k)$  denote, respectively, the hypermagnetic power spectrum and the traceless projector

$$P_B(k) = \mathcal{C}(\delta) H_1^4 \left( \frac{k}{k_1} \right)^{n_B-1} e^{-2 \frac{k^2}{k_\sigma^2}}, \quad P_{ij}(k) = \left( \delta_{ij} - \frac{k_i k_j}{k^2} \right). \quad (17)$$

In Eq. (17)  $\mathcal{C}(\delta) = 2^{2\delta-1} \Gamma^2(\delta) / \pi^2$  and

$$\delta = \frac{3\alpha - 1 + \epsilon(1 - 2\alpha)}{2(1 - \epsilon)}, \quad n_B = \frac{7 - 3\alpha - \epsilon(7 - 2\alpha)}{1 - \epsilon}, \quad k_1 = \frac{1}{\tau_1}. \quad (18)$$

In Eq. (17)  $k_\sigma$  is the conductivity wave-number, i.e.  $k_\sigma^{-2} = \int d\tau / (4\pi\sigma)$ . The wave-numbers  $k_1$  and  $k_\sigma$  can be also usefully expressed, within a comoving coordinate system, in units of  $\text{Mpc}^{-1}$ :

$$k_1 = 1.1 \times 10^{24} (\epsilon \mathcal{P}_\mathcal{R})^{1/4} \text{Mpc}^{-1}, \quad k_\sigma = 1.55 \times 10^{12} \left( \frac{h_0^2 \Omega_{b0}}{0.023} \right)^{1/2} \left( \frac{h_0}{0.7} \right)^{1/2} \text{Mpc}^{-1}, \quad (19)$$

where  $\epsilon$  is the slow-roll parameter already encountered in Eq. (8) and  $\mathcal{P}_\mathcal{R} \simeq 2.35 \times 10^{-9}$  is the inflationary power spectrum of curvature perturbations evaluated at the pivot scale  $k_p = 0.002 \text{Mpc}^{-1}$  and estimated according to the WMAP data alone [15]. The wave-numbers of Eq. (19) indeed correspond to very short wavelengths as it can be appreciated by comparing them to the comoving wave-number corresponding to the Hubble radius, i.e.  $k_0 = 2.33 \times 10^{-4} (h_0/0.7) \text{Mpc}^{-1}$ . The spectrum of Eq. (17) holds for  $k < k_1$ . But since the exponential fall-off triggered by the finite value of the conductivity becomes relevant already at  $k \simeq k_\sigma$  the power-law behaviour is only verified for sufficiently small wave-numbers  $k < k_\sigma$ . The two-point function of Eq. (16) has been computed by quantizing the system in the Coulomb gauge and by solving the resulting evolution equations in the Heisenberg representation. The final result (16) can also be expressed as a statistical condition on the (classical) Fourier amplitudes

$$\langle B_i(\vec{k}) B_j^*(\vec{p}) \rangle = \frac{2\pi^2}{k^3} P_B(k) P_{ij}(k) \delta^{(3)}(\vec{k} - \vec{p}). \quad (20)$$

The analytical calculation will now be corroborated by the appropriate numerical treatment where the transition from inflation to radiation is parametrized by

$$a(\tau) = a_1 (x + \sqrt{x^2 + 1}), \quad g^2 \lambda(x) = \left( \frac{2\sqrt{x^2 + 1}}{\sqrt{x^2 + 1} + x} \right)^{\frac{3\alpha}{2}}, \quad x = \frac{\tau}{\tau_1}, \quad (21)$$

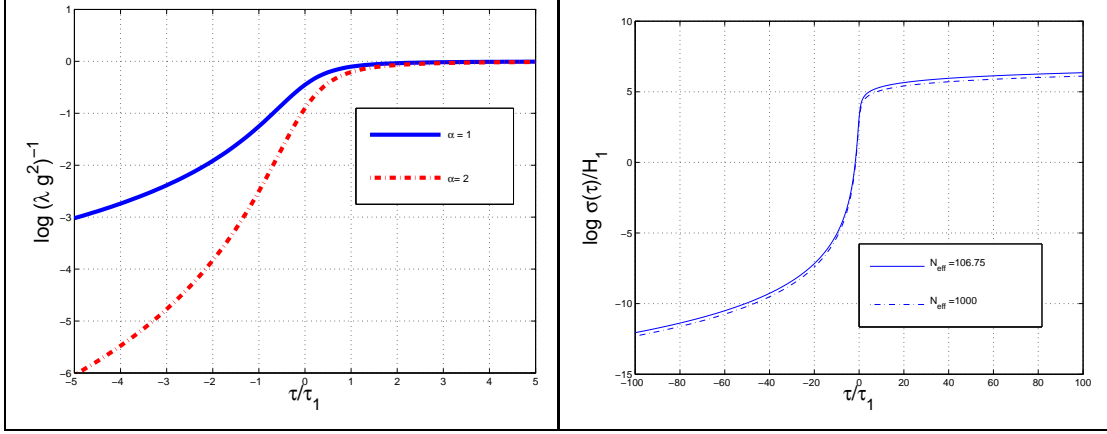


Figure 1: The evolution of  $\lambda$  (plot at the left) and of  $\sigma$  (plot at the right) is reported for different parameters of the model.

where  $g$  denotes the hypercharge coupling constant. The time  $\tau_1$  controls the duration of the transition regime: for  $\tau \ll -\tau_1$ ,  $\lambda \simeq (-\tau)^{3\alpha}$  as implied (to leading order in the slow-roll corrections) by the third relation in Eq. (9) in conjunction with Eq. (8). Similarly, if  $\tau \ll -\tau_1$  the scale factor appearing in Eq. (21) goes as  $a(\tau) \simeq (-\tau_1/\tau)$  (quasi de-Sitter expansion). Conversely, if  $\tau \gg \tau_1$ ,  $a(\tau) \simeq (\tau/\tau_1)$  (radiation dominated evolution) and  $g^2\lambda \rightarrow 1$ . The evolution of  $\lambda$  is graphically illustrated in Fig. 1) (plot at the left). The time evolution of the conductivity can be modeled as

$$\sigma_c(x) = \frac{T_{\text{rh}}}{\alpha} \theta(x), \quad \theta(x) = \frac{1}{8} \left( 1 + \frac{x}{\sqrt{x^2 + 1}} \right)^3, \quad (22)$$

where  $\theta(x)$  is a smooth representation of the Heaviside step function. Notice that the rationale for the third power stems from the fact that  $\sigma_c(\tau)$  should vanish fast enough for  $\tau \ll -\tau_1$ . The graphic illustration of the evolution of  $\sigma$  is reported in Fig. 1 (plot at the right). When the electroweak symmetry is unbroken the conductivity  $\sigma_c$  is of the order of  $T/\alpha$  where  $\alpha = g^2/4\pi$  and  $T$  is the temperature at the corresponding epoch. More accurate estimates of this quantity exist (see, for instance, [12] and [16]) and they agree, up to numerical factors, with the figures used in the present paper. In fact,  $\sigma_c$  is anyway much larger than the Hubble rate at the corresponding epoch. By relying on the assumption that all the inflaton energy density is efficiently converted into radiation energy density and by assuming a generic number  $N_{\text{eff}}$  of relativistic degrees of freedom  $T_{\text{rh}}$  can be estimated as

$$\frac{T_{\text{rh}}}{H_1} = \left( \frac{45}{4\pi^4 N_{\text{eff}}} \right)^{1/4} (\epsilon \mathcal{P}_{\mathcal{R}})^{-1/4}, \quad \mathcal{P}_{\mathcal{R}} = \frac{8}{3} \frac{V}{\epsilon M_{\text{P}}^4} \equiv \frac{1}{24\pi^2} \frac{V}{\epsilon \overline{M}_{\text{P}}^4}, \quad (23)$$

where the slow-roll equation  $3H_1^2 \overline{M}_{\text{P}}^2 \simeq V$  has been used. Even if  $N_{\text{eff}} = 106.75$  in the



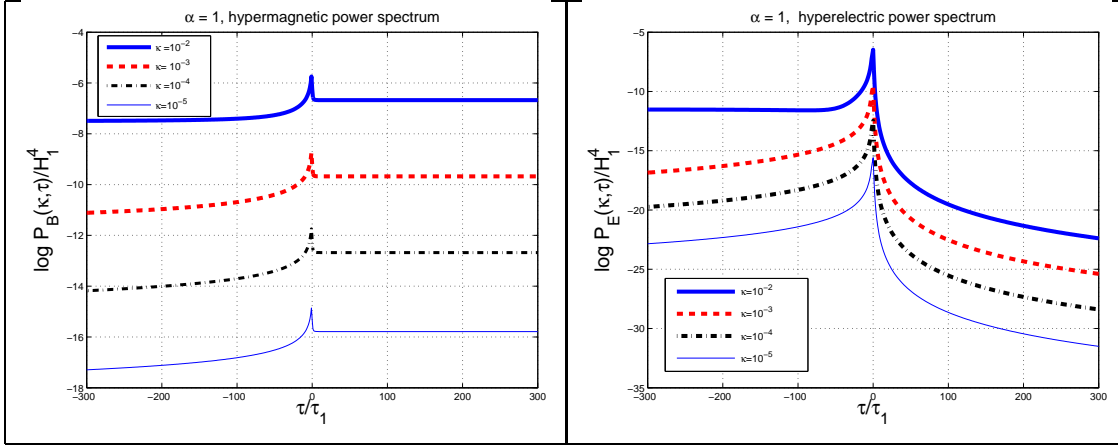


Figure 2: The numerical result for the evolution of the hypermagnetic and hyperelectric power spectra is illustrated on a semi-logarithmic scale.

standard model, a drastic variation of one order of magnitude does not affect crucially  $\sigma$  (see also Fig. 1). Recalling that  $\sigma(\tau) = \sigma_c(\tau)a(\tau)$  the evolution of the mode function in the presence of the Ohmic terms

$$f_k'' + \frac{4\pi\sigma}{\lambda} f_k' + \left\{ k^2 - \left[ \frac{(\sqrt{\lambda})''}{\sqrt{\lambda}} + \frac{4\pi\sigma}{\lambda} \frac{(\sqrt{\lambda})'}{\sqrt{\lambda}} \right] \right\} f_k = 0, \quad (24)$$

can be solved in the smooth background provided by Eqs. (21) and (22). Imposing quantum mechanical initial conditions on  $f_k$  (i.e.  $f_k = e^{-ik\tau}/\sqrt{2k}$  for  $\tau \rightarrow -\infty$ ) the hypermagnetic and hyperelectric power spectra can be obtained and the results are summarized in Fig. 2 and in the left plot of Fig. 3. According to Eqs. (17) and (18), if  $\alpha = 1$  (up to slow-roll corrections)  $n_B \simeq 4$ . Similarly, if  $\alpha = 2$ ,  $n_B \simeq 1$  and the magnetic power spectrum is nearly scale-invariant. In Fig. 2 the hyperelectric and hypermagnetic power spectra have been numerically computed in the case  $\alpha = 1$  and for different values of  $\kappa = k\tau_1$ , i.e. the comoving wave-number in units of the transition time  $\tau_1$ . The initial integration time  $x_i = \tau_i/\tau_1$  depends on the mode and it is chosen in such a way that  $\kappa x_i > 1$  at  $x_i$  so that each mode starts its evolution inside the Hubble radius. By comparing the corresponding values of  $\kappa$  in the left and right plots of Fig. 2 the hypermagnetic power spectrum is amplified while the hyperelectric power spectrum is exponentially suppressed. In Fig. 2 (plot at the left) the magnetic power spectrum is reported for different values of the wave-number. The amplitude increases with  $\kappa$ , which is exactly what we expect in the case of  $\alpha = 1$  where the magnetic power spectrum should scale, approximately, as  $\kappa^{n_B-1}$  with  $n_B = 4$ . In Fig. 3 (plot at the left) a more detailed comparison is illustrated. The starred points correspond to results of the numerical integration for different values of the  $\kappa$  while the dashed line

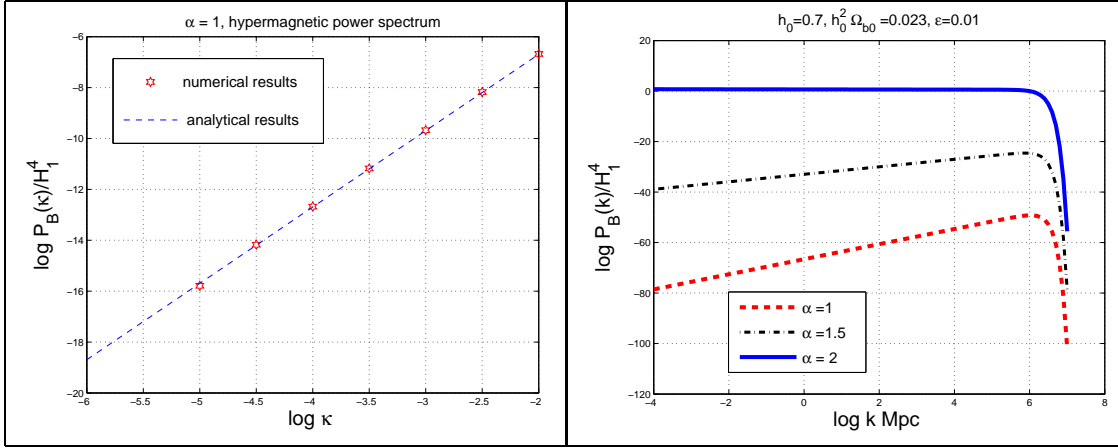


Figure 3: Comparison between analytical and numerical results in the case  $\alpha = 1$  and  $\epsilon = 0.01$  (plot at the left). The hypermagnetic spectrum as a function of the comoving wave-number in units of  $\text{Mpc}^{-1}$  (plot at the right).

corresponds to the analytical result. From Eqs. (17) and (18), in the case  $\delta = 1$ , we obtain

$$\log \left[ \frac{P_B(\kappa)}{H_1^4} \right] = \log 2 - 2 \log \pi + \frac{3 - 4\epsilon}{1 - \epsilon} \log \kappa, \quad (25)$$

where we identified  $k_1 \simeq \tau_1^{-1}$  so that  $k/k_1 \simeq \kappa$ . The dashed line in the left plot of Fig. 3 is not a fit but it is the result of the analytical expectation. Similar agreement is reached for different values of  $\alpha$ . Consequently, the analytical results based on the sudden approximation in conjunction with the matching conditions expressed by Eq. (15) are in good agreement with the numerical integration across a smooth transition of the same system of equations.

When the hypermagnetic fields will reenter the Hubble radius (prior to equality but after neutrino decoupling, taking place around the MeV) the electroweak symmetry is already broken. The non-screened vector modes of the hypercharge field will project on the electromagnetic fields as  $\mathcal{A}_i^{\text{em}} = \cos \theta_w \mathcal{Y}_i$ . The final magnetic power spectrum can then be presented (see Fig. 3, plot at the right) in units of  $H_1^4$ , i.e. the fourth power of the Hubble rate at the end of inflation. A more physical measure of the value of the obtained magnetic fields is the radiation energy density. The magnetic power spectrum in units of the radiation background is then

$$\frac{P_B(k)}{8\pi\rho_\gamma} = \pi \cos^2 \theta_w \mathcal{C}(\delta) \epsilon \mathcal{P}_{\mathcal{R}} \left( \frac{k}{k_1} \right)^{n_B-1}, \quad (26)$$

where both  $n_B$  and  $\delta$  depend upon the slow-roll parameter  $\epsilon$ . Since [15]  $\mathcal{P}_{\mathcal{R}} \simeq 2.35 \times 10^{-9}$ , in the scale-invariant limit Eq. (26) is of the order of  $10^{-10}$ . Consequently, the present

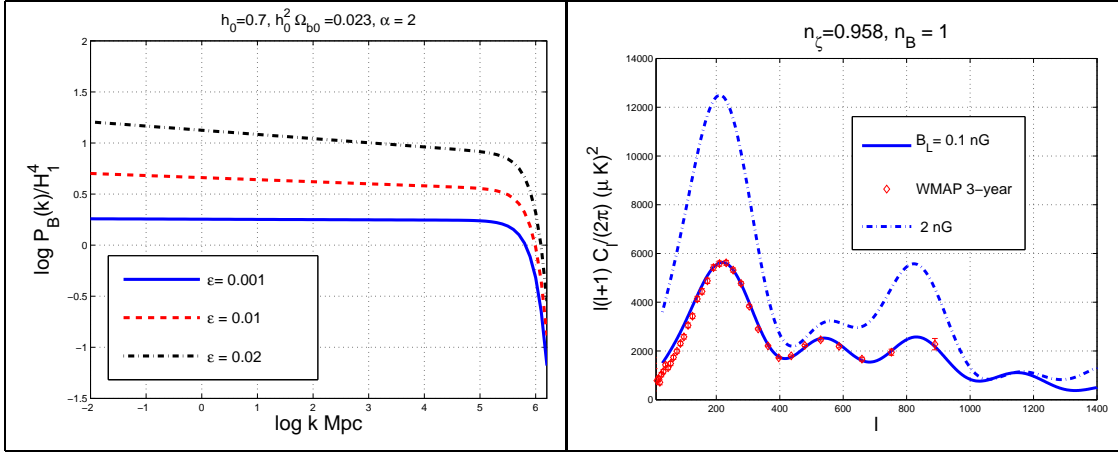


Figure 4: The hypermagnetic power spectrum for different choices of the parameters and as a function of the comoving wave-number in units of  $\text{Mpc}^{-1}$  (plot at the left). The temperature autocorrelations of the CMB anisotropies computed in the nearly scale-invariant limit according to the technique described in [10] (see, in particular, third reference).

value of the magnetic field is of order 0.1–0.01 nG with a theoretical error that depends upon  $\epsilon$  (which should be smaller than about 0.05 according to current experimental data<sup>7</sup>).

The results of Eq. (26) can also be illustrated by regularizing the magnetic field over a typical comoving scale  $L$  by means of a Gaussian window function in Fourier space [10, 18]. Denoting as  $B_L$  the regularized magnetic field over the comoving scale  $L = 2\pi/k_L$  we will have, in the nearly scale-invariant limit and at the time of the collapse of the protogalaxy,

$$\left(\frac{B_L}{\text{nG}}\right) \simeq 0.1 \left(\frac{\epsilon}{0.01}\right)^{1/2} \left(\frac{\mathcal{P}_{\mathcal{R}}}{2.35 \times 10^{-9}}\right)^{1/2}. \quad (27)$$

The magnetic energy density in units of the radiation background can be expressed, in this case, as

$$\overline{\Omega}_{\text{BL}} = \frac{B_L^2}{8\pi\rho_\gamma} = 7.56 \times 10^{-9} \left(\frac{B_L}{\text{nG}}\right)^2, \quad (28)$$

where the pivot value of  $B_L$  has been taken at the epoch of gravitational collapse of the protogalaxy. It is customary to require, for a successful magnetogenesis [11], that<sup>8</sup>  $\overline{\Omega}_{\text{BL}} > 10^{-34}$ , or, more realistically  $\overline{\Omega}_{\text{BL}} > 10^{-24}$ .

<sup>7</sup>It is possible to obtain an upper bound on  $\epsilon$  by analyzing, for instance, CMB and large-scale structure data within a  $\Lambda\text{CDM}$  model containing also a tensor component. The analysis will then lead to an upper limit on the ratio between tensor and scalar power spectra which can be translated into an upper limit on  $\epsilon$ . The combination of WMAP [15] data and the data of the Sloan Digital Sky Survey [17] would lead, for instance to  $\epsilon \lesssim 0.02$

<sup>8</sup>The first of these two figures stems from the (overoptimistic) requirement that the galactic dynamo

Equation (27) is compatible with a galactic magnetic field of the order of the  $\mu\text{G}$ . During the process of collapse the magnetic flux is frozen into the plasma element thanks to the large value of the conductivity. The mean matter density increases, during collapse, from its critical value (i.e.  $\rho_{\text{cr}} = 1.05 \times 10^{-5} h_0^2 \text{GeV}/\text{cm}^3$ ) to a final value  $\rho_f$  value which is 5 to 6 orders of magnitude larger than  $\rho_c$ . The magnetic field after collapse will then be

$$B_{\text{gal}} = \left(\frac{\rho_f}{\rho_c}\right)^{2/3} B_L \simeq \left(\frac{\epsilon}{0.01}\right)^{1/2} \left(\frac{\mathcal{P}_{\mathcal{R}}}{2.35 \times 10^{-9}}\right)^{1/2} \mu\text{G}. \quad (29)$$

Over present length-scales much larger than the Mpc the magnetic fields, in this model, will be (today) smaller than the nG since these regions did not benefit of the compressional amplification. Within this lore the magnetic fields in clusters could be produced by magnetic reconnection from the ones of the galaxies but the experimental uncertainty in their correlation scale [3] does not allow a definite statement. If the spectrum of the primeval field is not nearly scale-invariant its amplitude over a comoving Mpc scale will be smaller (see right plot of Fig. 3) and, consequently, a non negligible dynamo action will be required for the phenomenological relevance of the obtained result. In this second scenario the cluster magnetic field might be related to the way the dynamo is saturated.

In a series of papers a semi-analytical technique has been developed for the evaluation of the temperature autocorrelations (see, in particular, the third reference in [10]). Since in the present model the cross-correlation between magnetic and adiabatic contribution vanishes the temperature cross-correlations are given, for multipoles  $\ell < 30$  by the following generalization of the Sachs-Wolfe plateau:

$$C_\ell^{\text{(SW)}} = \left[ \frac{\mathcal{P}_{\mathcal{R}}}{25} \mathcal{Z}_1(n, \ell) + \frac{\epsilon^2 \mathcal{P}_{\mathcal{R}}^2}{400} R_\gamma^2 \mathcal{Z}_2(n_B, \ell) \right], \quad (30)$$

$$\mathcal{Z}_1(n, \ell) = \frac{\pi^2}{4} \left(\frac{k_0}{k_p}\right)^{n-1} 2^n \frac{\Gamma(3-n)\Gamma\left(\ell + \frac{n-1}{2}\right)}{\Gamma^2\left(2 - \frac{n}{2}\right)\Gamma\left(\ell + \frac{5}{2} - \frac{n}{2}\right)}, \quad (31)$$

$$\mathcal{Z}_2(n_B, \ell) = \frac{\pi^2}{2} 2^{2(n_B-1)} \mathcal{F}(n_B) \left(\frac{k_0}{k_1}\right)^{2(n_B-1)} \frac{\Gamma(4-2n_B)\Gamma(\ell+n_B-1)}{\Gamma^2\left(\frac{5}{2}-n_B\right)\Gamma(\ell+3-n_B)}, \quad (32)$$

$$\mathcal{F}(n_B) = \frac{4\pi^2}{27} \mathcal{C}^2(\delta) \frac{(7-n_B)}{(n_B-1)(5-2n_B)}, \quad n_B > 1, \quad (33)$$

where  $n$  denotes the spectral index of the adiabatic mode<sup>9</sup>. If  $n_B \simeq 1$  the function (33) is so efficient to amplify the protogalactic field by one e-fold for each galactic rotation. Strictly speaking this argument only applies to spiral galaxies. The second requirement takes into account the possible early saturation of galactic dynamo and it is still rather optimistic (see, for instance, the second reference of [1] for a discussion).

<sup>9</sup>For the numerical estimate of Fig. 4,  $n$  will be taken to be 0.958 which is the best fit value obtainable by analyzing the WMAP data alone [15].

contains the logarithm of the infra-red cut-off.

At smaller angular scales (i.e.  $\ell > 100$ ) the temperature autocorrelations can be obtained, within the scheme of [10] (third reference) by computing numerically four integrals and the results for multipoles compatible with the Doppler oscillations are reported in Fig. 4 (plot at the right). When  $B_L \simeq 0.1$  nG the structure of the Doppler oscillations is not altered (see also [10] for a model-independent discussion).

So far it has been assumed that the decay rate of the inflaton and of the spectator fields were comparable, i.e.  $\Gamma_\psi \simeq \Gamma_\varphi$ . It can also happen that the spectator field decays later than the inflaton. The predicted slopes of the magnetic power spectra will not be modified for comoving scales of the order of the Mpc. However, shorter wavelengths can be affected if the decay of  $\psi$  is delayed. In the latter case since  $\psi_* < \overline{M}_P$ , the ratio between the energy density of  $\psi$  and the radiation background (produced by the inflaton decay) will grow, after inflation. The fluctuations of the spectator field may then represent a further source of curvature perturbations. If the inflationary Hubble rate is much smaller than  $10^{-5}\overline{M}_P$  the fluctuations of  $\psi$  will eventually become the dominant source of curvature perturbations as noticed in the context of the so-called curvaton scenario [19]. In the opposite case the two contributions will interfere. In the latter case the final spectrum of curvature perturbations can be computed, for different post-inflationary evolutions, as a function of  $\psi_*$ . This analysis can be carried on numerically with the techniques already exploited in [20]. The final result can be written in terms of the amplitude of the curvature perturbations at the pivot scale:

$$\mathcal{P}_R = \frac{1}{24\pi^2} \frac{V}{\overline{M}_P^4} \left[ \frac{1}{\epsilon} + f^2(\psi_*) \right], \quad f(\psi_*) = c_1 \left( \frac{\psi_*}{\overline{M}_P} \right) + c_2 \left( \frac{\overline{M}_P}{\psi_*} \right) \quad (34)$$

where  $c_1 = 0.13$  and  $c_2 = 0.25$ . In the limit  $f \rightarrow 0$  we recover the result of Eq. (23). In the case  $f \neq 0$  the curvature fluctuations induced by  $\psi$  may mix, in the Sachs-Wolfe plateau, with the component induced by the inflaton fluctuations. In some cases there could even be a correlation term. As argued in [20] (second reference) these results strongly depend upon  $W(\psi)$  being quadratic and not, for instance quartic. In spite of the details of the post-inflationary history Eq. (34) suggests a possible violation of the consistency relation which would become, in the case of Eq. (34),  $r_T = 16\epsilon/[1 + 8f^2(\psi_*)\epsilon]$  having defined  $r_T = \mathcal{P}_T/\mathcal{P}_R$ , i.e. the ratio between the tensor and the scalar power spectra. This prediction would allow, in principle, to distinguish observationally the situations where the spectator field decays during reheating or later. We leave for a forthcoming paper the detailed analysis of this and other cases [21].

The main goal of the present study has been to demonstrate, within conventional inflationary scenarios, the viability of a class of magnetogenesis models that do not require a strong dynamo action and that are compatible, at the same time, with the direct bounds

stemming from the analysis of the CMB anisotropies. The foreseeable improvement of the quality of CMB data stimulates the effort of more accurate calculations of the impact of a magnetized plasma upon the various CMB observables. As explicitly demonstrated in this paper is possible to construct viable magnetogenesis models which have well defined CMB signatures. Since theoretical prejudices (and diatribes) are not a decisive proof for the existence (or not existence) of pre-recombination magnetic fields, it is wise pursue the development of model-independent tools for accurate analyses of magnetized CMB anisotropies, as suggested by the present investigation. Indeed, forthcoming satellite experiments may turn some of the present speculations in more solid scientific statements either in favour or against the primordial hypothesis.

## References

- [1] Ya. B. Zeldovich, A. A. Ruzmaikin, and D.D. Sokoloff, *Magnetic Fields in Astrophysics* (Gordon and Breach Science, New York, 1983); M. Giovannini, Int. J. Mod. Phys. D **13**, 391 (2004).
- [2] R. Beck, A. Brandenburg, D. Moss, A. Skhurov, and D. Sokoloff *Annu. Rev. Astron. Astrophys.* **34**, 155 (1996); R. Beck, Astron.Nachr. **327**, 512 (2006);
- [3] C. L. Carilli and G. B. Taylor, Ann. Rev. Astron. Astrophys. **40**, 319 (2002); T.E. Clarke, P.P. Kronberg and H. Böhringer, Astrophys. J. **547**, L111 (2001).
- [4] P. P. Kronberg, S. Habib and Q. W. Dufton, Astrophys. J. **637**, 19 (2006); P. P. Kronberg, Rep. Prog. Phys. **57**, 325 (1994).
- [5] J. Abraham *et al.* [Pierre Auger Collaboration], Science **318**, 938 (2007).
- [6] M. Aglietta *et al.* [Pierre Auger Collaboration], Astropart. Phys. **27**, 244 (2007)
- [7] E. Harrison, Phys. Rev. Lett. **18**, 1011 (1967); Mon. Not. R. Astr. Soc. **147**, 279 (1970).
- [8] A. Brandenburg and K. Subramanian, Phys. Rept. **417**, 1 (2005); A. Lazarian, E. Vishniac, and J. Cho, Astrophys. J. **603**, 180 (2004); Lect. Notes Phys. **614**, 376 (2003).
- [9] M. Giovannini, Class. Quant. Grav. **23**, R1 (2006); K. Subramanian, Astron.Nachr. **327**, 399 (2006); T. Kahniashvili, New Astron. Rev. **50**, 1015 (2006).
- [10] M. Giovannini, Phys. Rev. D **73**, 101302 (2006); Phys. Rev. D **74**, 063002 (2006); PMC Phys. A **1**, 5 (2007).

- [11] M. S. Turner and L. M. Widrow, Phys. Rev. D **37**, 2743 (1988); B. Ratra, Astrophys. J. **391**, L1 (1992); M. Gasperini, M. Giovannini and G. Veneziano, Phys. Rev. Lett. **75**, 3796 (1995); M. Giovannini, Phys. Rev. D **62**, 123505 (2000); Phys. Rev. D **64**, 061301 (2001); K. E. Kunze, Phys. Lett. B **623**, 1 (2005); arXiv:0710.2435 [astro-ph].
- [12] M. Giovannini and M. E. Shaposhnikov, Phys. Rev. D **57**, 2186 (1998); M. Giovannini, Phys. Rev. D **61**, 063004 (2000).
- [13] M. K. Gaillard and B. Zumino, Nucl. Phys. B **193**, 221 (1981).
- [14] L. H. Ford, Phys. Rev. D **31**, 704 (1985).
- [15] D. N. Spergel *et al.* [WMAP Collaboration], Astrophys. J. Suppl. **170**, 377 (2007); L. Page *et al.* [WMAP Collaboration], Astrophys. J. Suppl. **170**, 335 (2007).
- [16] J. Ahonen and K. Enqvist, Phys. Lett. B **382**, 40 (1996); M. Giovannini, Phys. Rev. D **61**, 063502 (2000).
- [17] D. J. Eisenstein *et al.* [SDSS Collaboration], Astrophys. J. **633**, 560 (2005); M. Tegmark *et al.* [SDSS Collaboration], Astrophys. J. **606**, 702 (2004).
- [18] A. Kosowsky, T. Kahniashvili, G. Lavrelashvili and B. Ratra, Phys. Rev. D **71**, 043006 (2005); A. Mack, T. Kahniashvili and A. Kosowsky, Phys. Rev. D **65**, 123004 (2002).
- [19] K. Enqvist and M. S. Sloth, Nucl. Phys. B **626**, 395 (2002); D. H. Lyth and D. Wands, Phys. Lett. B **524**, 5 (2002).
- [20] M. Giovannini, Phys. Rev. D **67**, 123512 (2003); V. Bozza, M. Gasperini, M. Giovannini and G. Veneziano, Phys. Rev. D **67**, 063514 (2003).
- [21] M. Giovannini, in preparation.